BULLETIN OF THE EARTHQUAKE
RESEARCH INSTITUTE
Vol. 57 (1982), pp. 239-262

12. Experimental Study of a Tsunami Generated by a Horizontal Motion of a Sloping Bottom.

By Sin'iti IWASAKI,
Earthquake Research Institute.
(Received April 30, 1982)

Abstract

A tsunami generated by a transient horizontal motion of a sloping bottom is discussed experimentally. The experiment was performed in a channel by varying three independent parameters S, L and τ, which represent the bottom slope near one end of the tank, the total horizontal displacement and the rise time of the bottom movement, respectively. About the maximum run-up of the water's edge, the following characteristics are found for moderate values of L and τ. 1) For S=1/1, the run-up height exhibits analogous behavior to the wave generated by the horizontal motion of a vertical wall. 2) For S$\leq$ 1/3, the run-up height is dominated by a vertical component of the horizontal displacement, namely, LS. 3) Wave characteristics are well described by a linear-long wave theory. 4) Unified interpretation is possible for three different mechanisms of wave generation; the vertical motion of a horizontal bottom, the horizontal motion of a vertical wall, and the horizontal motion of a sloping bottom.

1. Introduction

Tsunami generation is due to an external disturbance given on a boundary surface of an ocean. About this problem, various generating models have been examined both theoretically and experimentally. They are divided broadly into two categories; the vertical motion of a bottom in an ocean of constant depth (type A) and the horizontal motion of a vertical wall (type B). For the type A, KAJIURA (1963) discussed the general characteristics of generated waves on the basis of the time dependent Green's function. In particular, for the case of one-dimensional propagation of waves, KAJIURA (1970) showed a simple relation between the generated wave amplitude and various parameters of a uniform vertical bottom motion in the source area, provided that linear and long-wave approximations were valid. The maximum water level elevation, H, at the center of the generating area relative to the final displacement of the bottom is determined by a non-dimensional parameter:

the time ratio between the rise time τ of the bottom displacement and the travel time T for a gravity wave to propagate from the center to the edge of the bottom deformation. HAMMACK (1973), not using the long wave approximation, presented a wave disturbance in an integral form and gave similar relations as long as the size of the generating area is much greater than the water depth. He verified his theory by detailed experiments.

Studies of the type B were developed originally as a theory of wave maker (URSELL, DEAN and YU, 1959), and they were applied to the problem of wave agitation in a harbor due to periodic forcing of a vertical wall due to seismic waves (HWANG and LEE, 1975) and to the tsunami problem due to a transient movement of a vertical wall (NODA, 1970; DAS and WIEGEL 1972). Assuming a long wave approximation, NODA (1970) gave the relation for the maximum amplitude H of generated waves as H/D=FR where D is the water depth, L is the horizontal displacement and FR is the Froud number defined by $(L/\tau)/\sqrt{gD}$ with g being the acceleration due to gravity and τ the time duration of the movement of a vertical wall.

Between the above two types of generation mechanisms, there are cases of wave generation by the movement of a sloping bottom (type C). In paticular, if an earthquake occurs in a coastal vicinity, the coastal sea bottom is expected to move horizontally and a tsunami may be generated and inundate the coastal land. Therefore, the estimation of the maximum run-up for this type of wave generation might be important. However, only a few studies have been conducted on this type of tsunami generation. GARCIA (1972) treated this kind of problem, but his main interest was not in the movement of the water's edge but a wave-form generated by the movement of a wall formed by an abrupt change in depth of the submarine topography. Therefore, his laboratory experiments were performed only over small parameter ranges and also he collected no data in the vicinity of the generating area in which we are most interested.

In this paper, the results of laboratory experiments concerning wave generation of the type C are presented and some theoretical discussions are made with emphasis on the following two aspects: 1) Estimation of the validity of a linear long wave theory in the near-field and at the water's edge in particular, and 2) Unified interpretation of behaviors of the maximum run-up caused by the three types of wave generation mechanisms mentioned above.

2. Experiment

Experimental equipments

A unique point in the present experiment is that a movable tank with a sloping bottom is used to reproduce the horizontal motion of ground. A schematic diagram and the dimensions of the experimental equipment are shown in Fig. 1. Some of these are described below.

A moving frame; the motion of a moving frame is controlled by a motor whose transmission can change its speed continuously. The stroke can also be changed continuously. Ranges of the period and the stroke are shown in Table 1. This system has a stopper which can stop the moving frame immediately at any desired spot.

A movable tank; a movable tank consists of two parts; a rectangular tube and a sloping wall. Four different sloping walls are used in this experiment; slopes (ratios of vertical to horizontal) are 1/1, 1/3, 1/5 and 1/10. The sloping wall has a plate in its rear side which plays the roll of joining the rectangular tube and the brass bar. The bar transmits the motion of the moving frame to the tank. In this way the motion of the movable tank is controlled by a moving frame, and, at the same time, the leakage of water from lateral sides of the sloping wall is completely prevented.

Wave height gauges; two types of wave height gauges are used. One is specifically made for the measurement of run-up near the water-edge. Two thin stainless wires are streched parallel to the sloping wall with

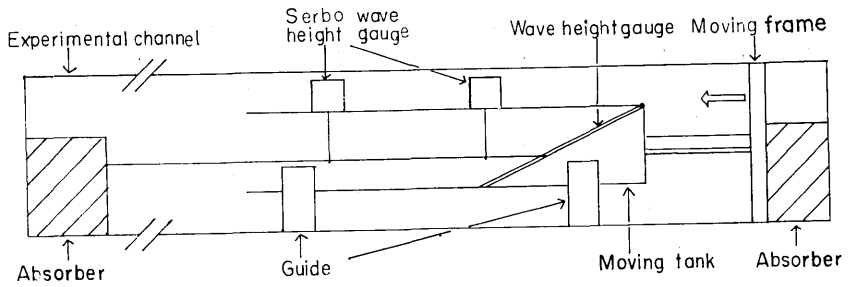

Experimental channel : 400X425X10,000 mm
Moving tank : 200X200X4,000 mm
Moving frame : Stroke 0～400 mm
Period 0.48～20.0 sec

Fig. 1. Schematic diagram and dimensions of experimental equipments.

Table 1. Ranges of parameters S, L, τ and FR. S denotes the slope of the sloping wall (vertical/horizontal), L the stroke, τ the rise time and FR the Froud number.

S	L (cm)	τ (sec)	$FR.=L/\tau\sqrt{gD}$
1/1	3	0.240~2.876	0.048~0.751
1/3	6 15	0.240~2.844	0.026~0.796
1/5	25 35	0.240~2.836	0.026~1.014
1/10	40	0.240~2.886	0.029~0.897

τ : rise time
D=6 cm

a clearance of 5 mm. It converts up-down motions of the water surface to the variation of voltage using the resistance of water. Therefore, calibration is necessary before and after each experimental run. The other is a Servo-wave-height-gauge. Throughout this experiment, the response speed of this gauge is maintained at 2.04 cm/sec. Thus, the wave with a peak to peak amplitude of up to 1 cm can be measured accurately as long as its period is over 0.49 sec.

Parameters

The ranges of three independent parameters S, L, τ and one composite parameter, FR, are shown in Table 1. S, L and τ denote the slope of a sloping wall, total horizontal displacement, and rise time (duration of the movement) respectively. FR (Froud number) is defined by $L/(\tau\sqrt{gD})$ with L/τ being the average moving speed of the sloping wall (horizontal displacement divided by the rise time), g is the acceleration of gravity and D the constant water depth beyond the sloping wall in the moving tank. The water depth is maintained at 6.0 cm for all experiments.

Experimental procedures

After the sloping wall and measuring instruments are set up, each set of experiments is performed following the procedures described in the diagram shown in Fig. 2.

Measurement and recording

The duration of motion of a moving frame (i. e., rise time)*, the run-up of the water's edge (H1), the surface elevation time histories at the outer edge of the sloping wall (H2), and the constant depth in the movable tank at a spot 15D from the outer edge of the sloping wall (H3) are measured and recorded by an x-y pen recorder. Various para-

* The period is measured by use of a rheostat. The stroke, another quantity to be determined, is measured in each run of experiments by a scale lay along the moving frame.

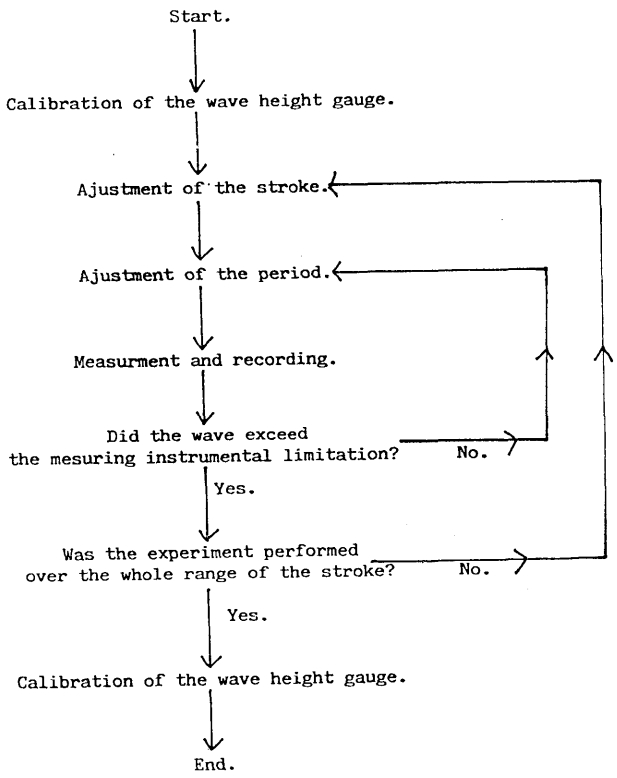

Fig. 2. Diagram showing experimental procedures.

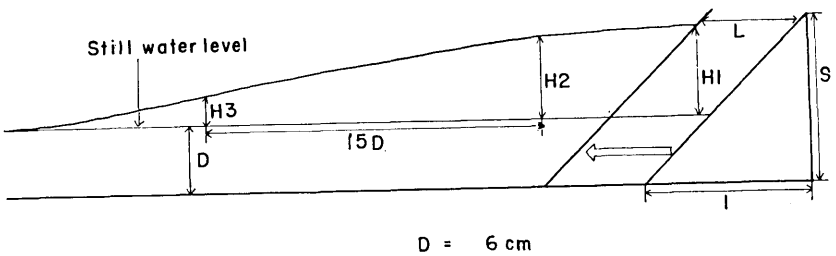

Fig. 3. Explanation of symbols.

meters are illustrated schematically in Fig. 3. H1, H2 and H3 are measured from a still water level. For example, the record of Run No. 120 is shown in Fig. 4, in which, from the bottom, time mark, time histories of wall displacement, H1, H2 and H3 are illustrated. Except for the actual values of amplitudes, H1 and H2 give the nearly the same wave characteristics; that is, first a crest is formed which is followed by a trough with the amplitude from one-third to one-fifth of the first crest and this

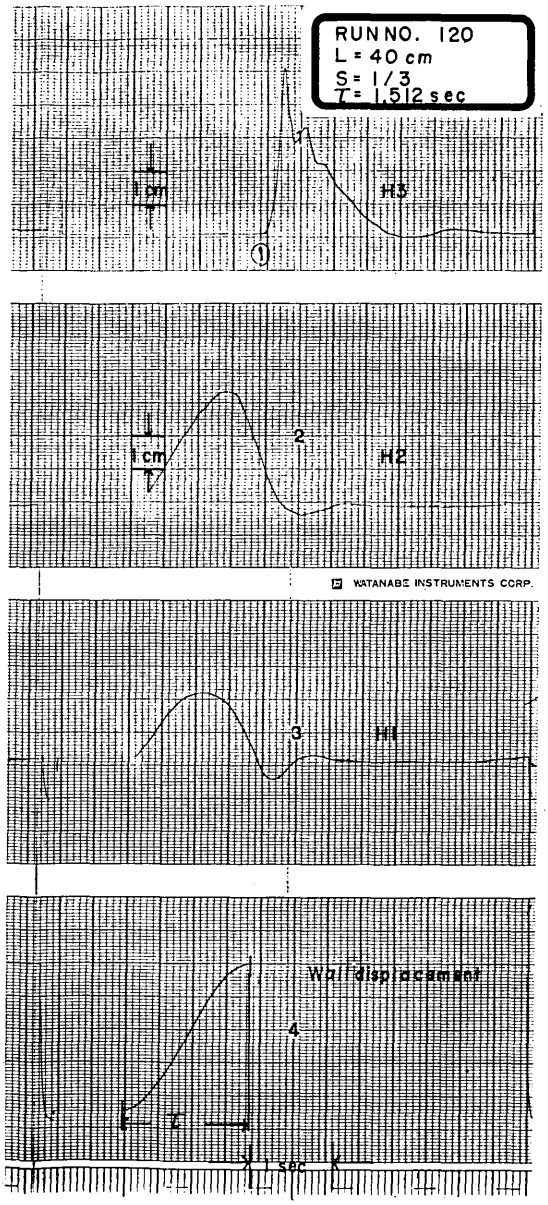

Fig. 4. A sample record. From the bottom, time mark, time histories of wall displacement, H1, H2 and H3.
Note: wall displacement and H1 are not to scale.

is then followed by a second crest with about the same amplitude as the trough. The wave form of H3 exhibits a distinctive non-linear and dispersive nature because of a large wave height compared to water

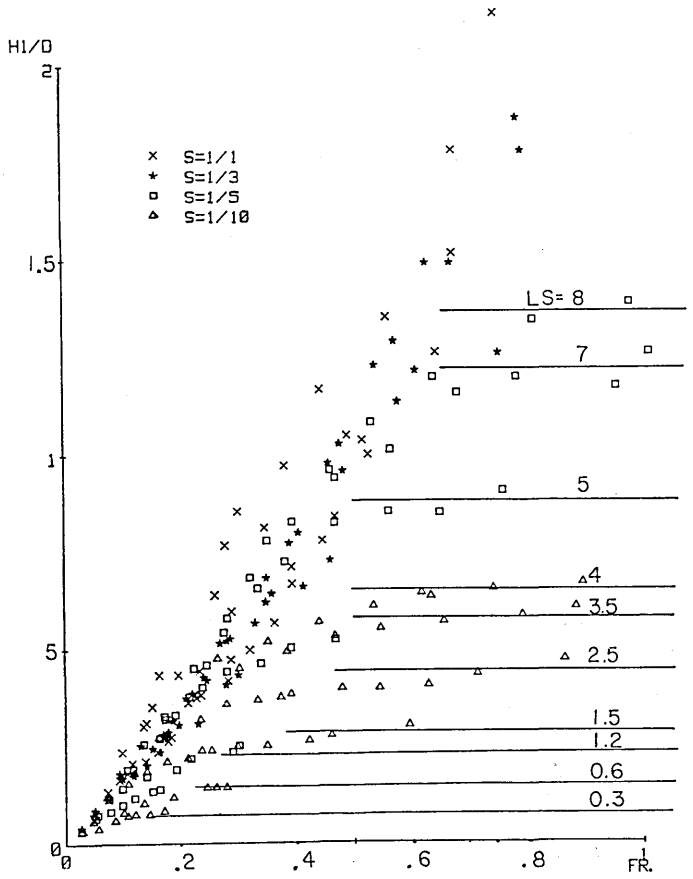

Fig. 5. Relative wave height H1/D as a function of FR.

depth in this case. The first crest values of H1, H2 and H3 are mainly analyzed, so that hereafter H1, H2 and H3 denote their maximum values unless so noted.

3. Experimental results

Relative wave heights at the water's edge, H1/D, are shown in Fig. 5. as a function of FR for several values of S. For S=1/1, H1/D is found to be proportional to FR. This tendency is expected theoretically for cases where the waves are generated by the horizontal motion of a vertical wall (NODA, 1970). For $S \lesssim 1/3$, it is found that H1/D is proportional to FR for small values of FR, but for large values of FR, H1/D approaches a constant value independent of FR. The values of H1/D at which H1/D become independent of FR are nearly proportional to the

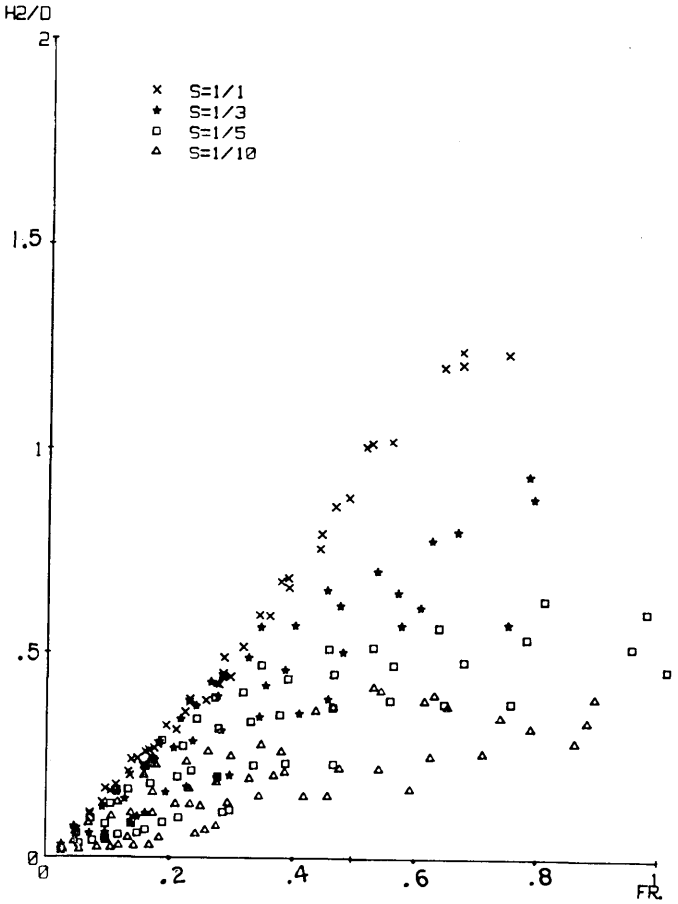

Fig. 6. Relative wave height H2/D as a function of FR.

vertical component of the displacement, namely, LS. Therefore, it is suggested that the maximum run-up is mainly governed by the vertical motion of the bottom for small S.

The relative wave height H2/D as a function of FR is shown in Fig. 6. The behaviors is analogous to the case of H1/D provided that H2/D is smaller than H1/D.

The relative wave height H3/D as a function of FR is shown in Fig. 7. Contrary to H1/D and H2/D shown in Fig. 5 and Fig. 6, there exists a maximum of H3/D in Fig. 7 for certain values of FR because of the occurrence of waves breaking before the arrival of waves at the location of H3. In particular, for S=1/1 waves break at a level of H3/D $\simeq$1.0. Since we are mainly concerned with wave characteristics within the region of wave generation, detailed analysis of H3/D is not under-

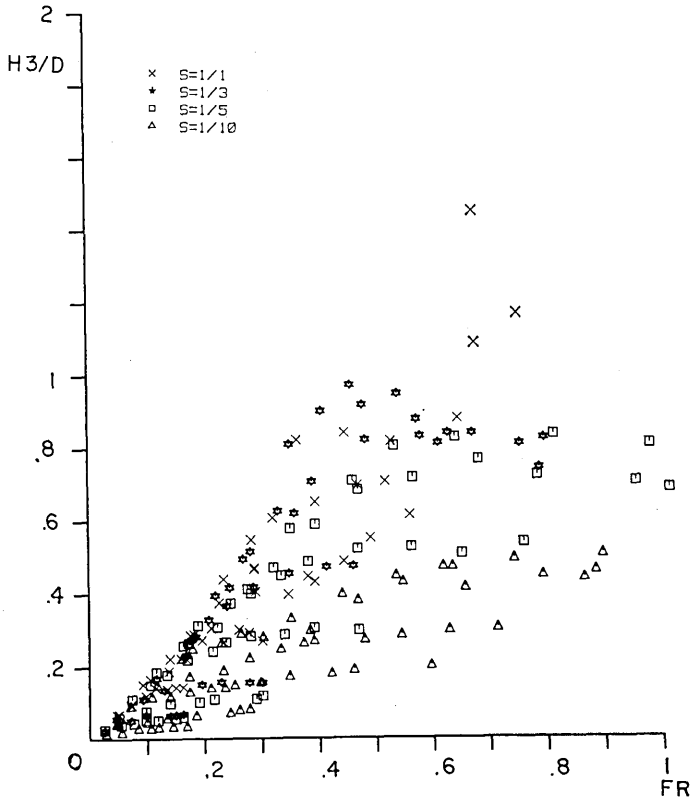

Fig. 7. Relative wave height H3/D as a function of FR.

taken. As is evident in Fig. 3 the wave pattern at the location of H3 in the parameter range of the present experiment exhibits dispersive and non-linear characteristics because sufficient travel time is available for the wave to deform by these effects.

4. Comparison of experimental results with a linear shallow water theory

From the analysis of the previous section, it is suggested that the maximum run-up is governed by the vertical displacement of a sloping bottom, LS, for small S. The wave generation by a vertical motion of a part of the bottom in a channel of constant depth is considered as a limiting case of $S \to 0$ in the present experiment. For this special case, it is known (HAMMACK, 1973) that the generation of wave is well described on the basis of a linear, shallow water theory provided the wave

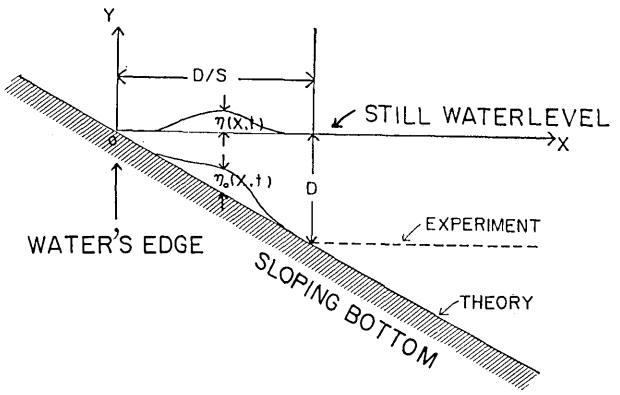

Fig. 8. Schematic drawing of the ground motion and the co-ordinate system.

generating area is large enough compared to the water depth. Thus, it is reasonable to use the linear long wave approximation to calculate the wave generated by the vertical displacement of a sloping bottom.

According to TUCK and HWANG (1972), the resulting surface elevation $\eta(x, t)$ above still water level when a vertical displacement $\eta_0(x, t)$ is given on a uniformly sloping bottom is given by

$$\eta(x,t)=\frac{2}{(gS)^{1/2}}\int_0^\infty J_0(2kx^{1/2})dk\int_0^\infty J_0(2k\xi^{1/2})d\xi \times\int_0^t \ddot{\eta}_0(\xi,\tau')\sin\left[(gS)^{1/2}k(t-\tau')\right]d\tau' \tag{1}$$

in the co-ordinate system indicated in Fig. 8, where g denotes the accerelation of gravity, S the slope of a sloping bottom, $J_0(z)$ the zero's order Bessel function of the first kind with argument z and $\ddot{\eta}_0$ the second time derivative of η_0.

In our experiment, the time history of the bottom displacement is well approximated by a straight line and the generating area is restricted to $0\leq x\leq D/S$. Thus, $\eta_0(x, t)$ is given by

$$\eta_0(x,t)=\begin{cases}(LS/\tau)t & ;\ 0\leq x\leq D/S,\quad 0\leq t\leq\tau\\ LS & ;\ 0\leq x\leq D/S,\quad \tau\leq t\\ 0 & ;\ D/S<x\quad ,\quad \text{for all } t\end{cases} \tag{2}$$

where τ denotes the rise time, and L the stroke (total horizontal displacement). Although the condition of a semi-infinite sloping bottom for the formula (1) is different from our experimental set up (see, Fig. 8),

the water surface disturbance is expected to be well represented by the formula at least for the early stage.

Substituting (2) for (1), $\eta_0(x, t)$ becomes δ-function at $t=0$ and $t=\tau$, and, (1) is separated into two parts:

$$\eta(x, t)=\eta_1-\eta_2 \tag{3}$$

where

$$\eta_i=(gS)^{-1/2}\int_0^\infty J_0(2kx^{1/2})dk\int_0^{D/S} J_0(2k\xi^{1/2})d\xi\times(LS/\tau)\cdot\sin[(gS)^{1/2}kt_i]\cdot H(t_i)$$

with $t_i=t$ (for $i=1$) or $t-\tau$ (for $i=2$) and $H(t_i)$ the Heaviside's step function.

Thus, the run-up $R(t)$ at the water's edge becomes

$$R(t)=\eta_1(0, t)-\eta_2(0, t) \tag{4}$$

where

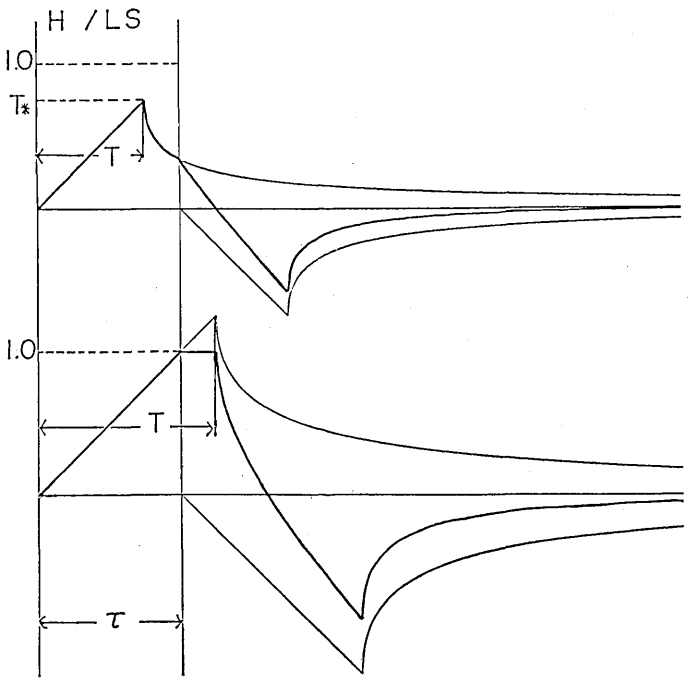

Fig. 9. Time histories of the relative wave elevation at the water's edge, $R(t)/LS$, under the linear long-wave approximation, for two cases, $T<\tau$ and $T>\tau$.

$$\eta_i(0,t)=2(gS)^{-1/2}(LS/\tau)(D/S)^{1/2}$$
$$\times\int_0^\infty k^{-1}J_1(2k(D/S)^{1/2})\sin\{(gS)^{1/2}kt_i\}\mathrm{H}(t_i)dk,\ i=1,\ 2. \tag{5}$$

An explicit form of $\eta_i(0,t)$ is given by

$$\eta_i(0,t)/(LS)=\begin{cases} T_i & \text{for } T_i\leq T^* \\ T_i-(T_i^2-T_*^2)^{1/2}, & \text{for } T_i>T^* \end{cases} \tag{6}$$

where $T_i=t_i/\tau$ and $T^*=T/\tau$ with $T=(D/S)/(\sqrt{gD}/2)$. It is noted that T is the time required for a disturbance to propagate from $x=0$ to $x=D/S$ with the long gravity wave speed. The time history of, $R(t)/(LS)$ is shown in Fig. 9 for two cases, $T<\tau$ and $T>\tau$.

From (6) the maximum run-up at the water's edge H1 is then given by

$$\mathrm{H1}/(LS)=\begin{cases} T^*, & \text{for } T^*<1.0 \\ 1.0, & \text{for } T^*\geq 1.0 \end{cases} \tag{7}$$

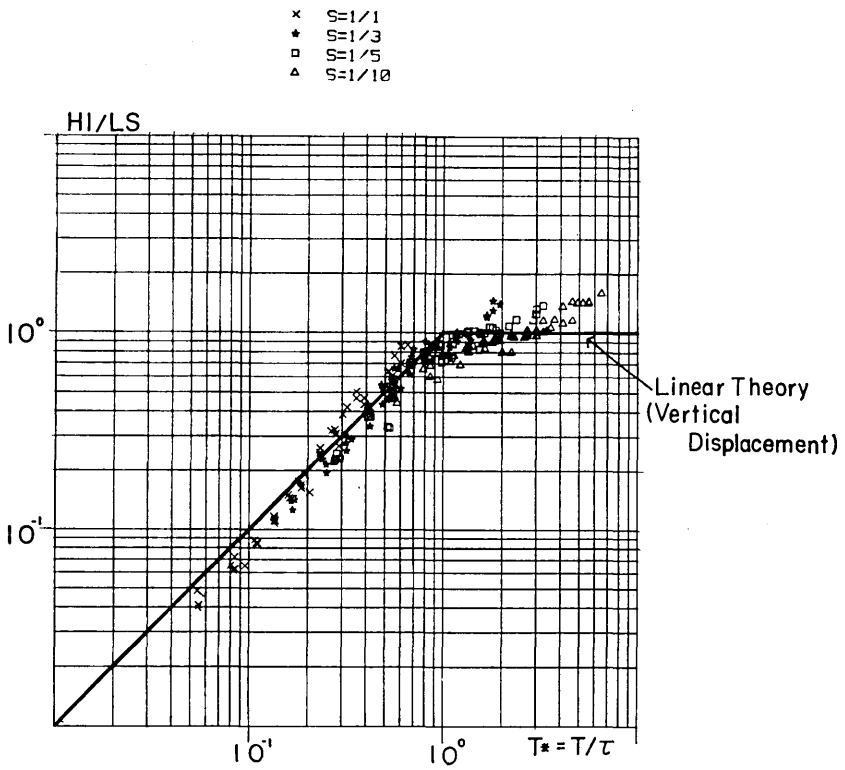

Fig. 10. Comparison of the observed maximum run-up (normalized by the vertical component of horizontal displacement, LS) with the prediction by the linear long-wave theory.

and the time t_m when the maximum occurs is

$$t_m=\begin{cases} T & , \quad \text{for} \quad T^*<1.0 \\ \tau & , \quad \text{for} \quad T^*\geq 1.0. \end{cases} \tag{8}$$

From (7) and (8), it is found that for $T^*<1.0$ (namely, for $T<\tau$) the maximum occurs during the sloping wall in motion. As T^* approaches 1, the occurrence of the maximum value moves towards the end of the rise time τ and for $T^*\geq 1.0$ (namely, for $T\geq\tau$) it is fixed at the end of the rise time. Since the maximum run-up at the water's edge always occurs on or before $t=T$, the prediction by (7) is not affected by the difference of the bottom configuration beyond $x=D/S$.

Comparison of the maximum run-up between the theory and the present experiment is made in Fig. 10 which shows clearly that the major characteristics of run-up is explained by the present simple theory, though some discrepancy is noted. Further discussion of Fig. 10 will be made later.

In Fig. 11 the time histories of run-up for various slopes are shown,

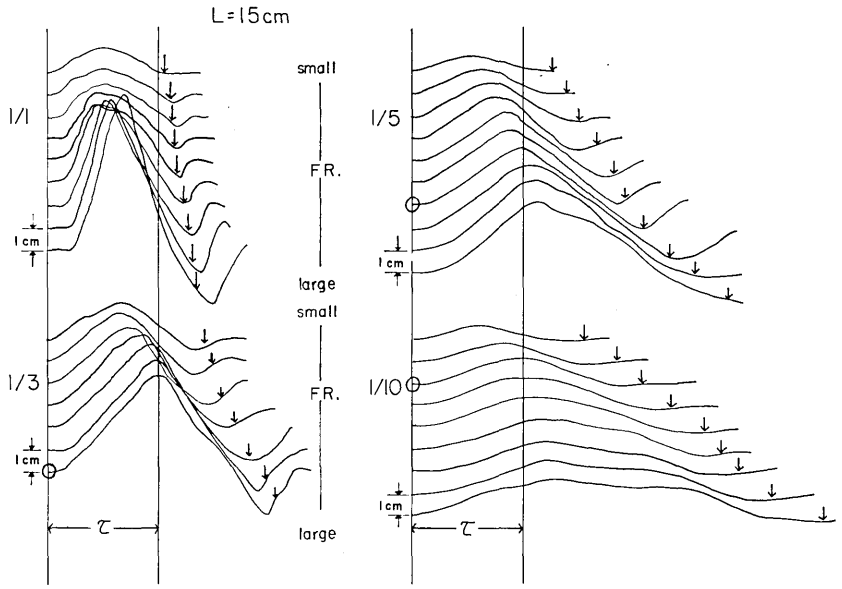

Fig. 11. Time histories of the observed run-up for various slopes in which the stroke is constant, L=15 cm. Time scale is normalized by the rise time τ. Circles on the ordinate indicate that, below these symbols, T^* is larger than 1.0 and arrows in the signature represent the expected trough occurrence by the linear long-wave theory.

in which the bottom displacement is constant, $L=15\,\mathrm{cm}$, and the time scale is normalized by the rise time. In each slope, figures are arranged from top to bottom in the order of the increasing FR, namely, the velocity of the moving frame from moderate to very large. Circles on the ordinate in Fig. 11 indicate that below these symbols T^* is larger than 1.0, and arrows on the signatures indicate the time of trough occurrence expected from the theory. For $S=1/1$, the experiment was made only over the range of T^* less than 1.0 because of instrumental difficulties. But, it is noticed that the position of the peak moves to the right as T^* inceases. For $S\leq 1/3$, the position of the peak also moves to the right for $T^*<1.0$ and fixed at the end of the rise time for $T^*\geq 1.0$. Both of these features are in agreement with the theory. The arrows, which indicate the theoretical trough position, deviate from experimental results, suggesting a discrepancy between the theory and the experiment. This is partly due to the presence of a constant depth channel in the experiment. For $S=1/1$, the positions of arrows are before the experimental trough occurrece, and for $S\leq 1/3$ the trough positions are after. However, it seems that if the slope is the same the arrows point to nearly the same relative positions with respect to actual trough independent of the Froud number. Amplitudes of both the initial crest and trough decrease with decreasing slopes as expected.

5. Unified interpretation of various generating mechanisms

Waves generated by the vertical motion of a bottom in an ocean of constant depth and by the horizontal motion of a vertical wall have already been discussed independently by various investigators. In this section, a unified interpretation of wave generation is attempted based on (7) by focusing attention on the maximum run-up at the edge of water.

The parameters shown in the ordinate and abscissa in Fig. 10 may be interpreted as follows:

$$\text{ordinate}: \mathrm{H1}/LS=[\text{the maximum run-up}]\,/\,[\text{vertical component of displacement}]$$

$$\text{abscissa}: T/\tau=\{(D/S)/(\sqrt{gD}/2)\}/\tau$$

$$=\left[\begin{array}{l}\text{the time required for a disturbance to}\\ \text{propagate from } x=0 \text{ to } x=D/S \text{ at the}\\ \text{speed of a long gravity wave}\end{array}\right]\Big/[\text{rise time}]$$

or

$$= \left[\begin{array}{l}\text{the time required for a disturbance to}\\ \text{propagate over the full length of the}\\ \text{generating area at the speed of a long}\\ \text{gravity wave}\end{array}\right] \Big/ [\text{rise time}].$$

Applying these interpretations, a unified understanding is possible for wave generation problems of the type A and type B in the following way. For a vertical motion of a bottom in an ocean of constant depth (type A), the relevant parameters (see, Appendix A) are the vertical displacement ζ_0, the size of the generating area b† and the rise time τ. Therefore, by replacing LS by ζ_0 and T by $b/\sqrt{gD}$, (7) can be transformed to the solution given by KAJIURA (1970) (see, Appendix A). On the other hand, for the case of a horizontal motion of a vertical wall, there is no explicit scale corresponding to the vertical displacement. However, according to the discussion in the section 3 and Appendix B, this case is found to be analogous to the case of $S=1/1$ so that we may put the approximate size of the generating area as D, namely, $T=D/\sqrt{gD}$, and the vertical displacement LS as L. Thus, (7) becomes the solution given

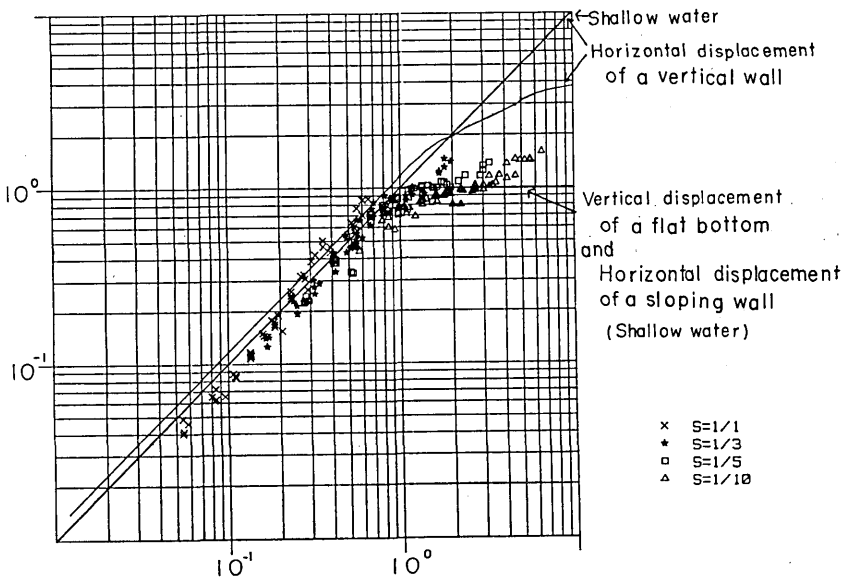

Fig. 12. Theoretical predictions by the three types of wave generation. Data of the present experiment are also plotted. Parameters to be assigned to both axes are shown in Table 2.

† As shown in Appendix A, the size of the generating area is 2b. But for the problems of run-up, we have to consider the case where a vertical wall is located at $x=0$. Thus, the size of the generating area is b.

Table 2. Parameters of the both axes of Fig. 12 for three types of wave generations.

Type	Parameters for the ordinater.	Parameters for the abscissa
A (Vertical motin of a flat bottom)	$H1/\zeta_0$	$b/(\tau\sqrt{gD})$
B (Horizontal motion of a vertical wall)	$H1/L$	$D/(\tau\sqrt{gD})$
C (Horizontal motion of a sloping wall)	$H1/LS$	$(D/S)/(\sqrt{gD/2})/\tau$

by NODA (1970) under the long-wave approximation (see, Appendix A).

Thick lines in Fig. 12 show the theoretically expected characteristics of the maximum run-up for the three types of wave generation, respectively. Parameters to be assigned to both axes are shown in Table 2. The maximum height H1 for the type A generation (KAJIURA, 1970) coincides perfectly with the theory for the sloping bottom (type C). Although the plotted data points for large parameter values of the abscissa is located between the theoretical lines for the horizontal displacement of a vertical wall (type B) and the vertical displacement of a horizontal bottom (type A), they approach the line expected of a vertical displacement as the slope becomes small. This trend may indicate the validity of these interpretations mentioned above.

An alternate formulation for the case of a sloping bottom is also possible, since in (7) the horizontal area related to the maximum run-up at the water's edge is limited to L*, the distance over which the influence of a water disturbance at the water's edge propagates during the rise time. If L^* is smaller than D/S, the length L^* is computed from the relation

$$\tau=\int_0^{L^*}(gSx)^{-1/2}dx$$

or $L^*=(1/4)gS\tau^2$. If we write the water depth at $x=L^*$ as $D^*(=L^*S)$ and define the average Froud number FRB as

$$\mathrm{FRB}=(L/\tau)/(L^*/\tau)=L/L^* \qquad (9)$$

then, for $L^*<D/S$ (or $T>\tau$), the second relation of (7) becomes

$$H1/D^*=\mathrm{FRB}. \qquad (10)$$

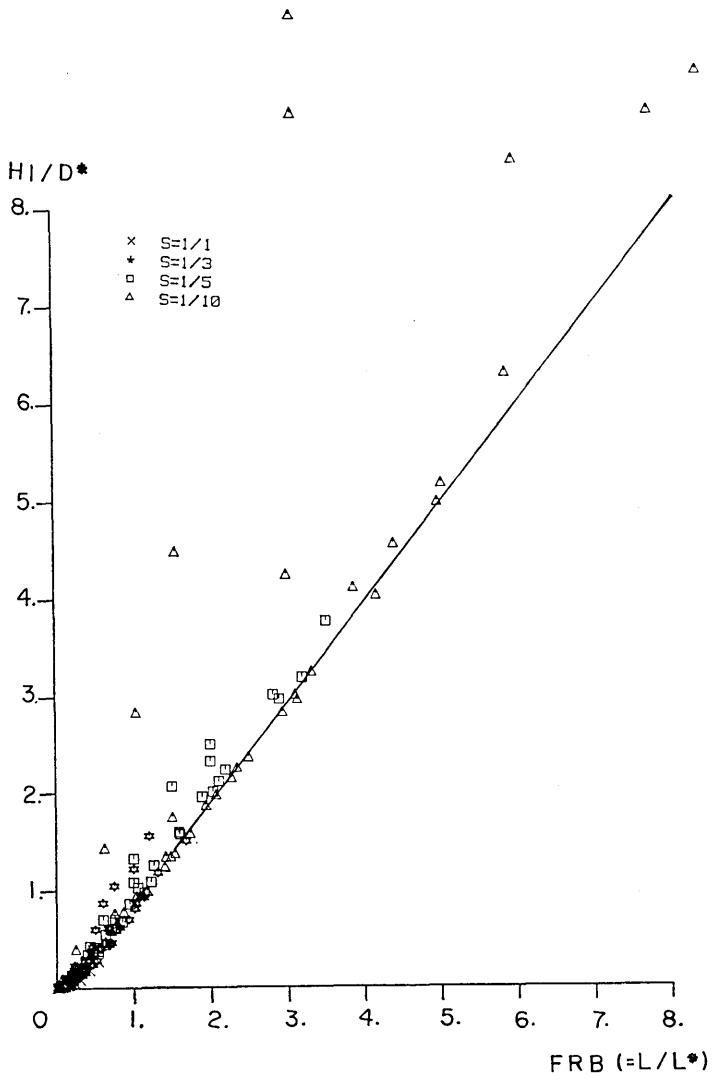

Fig. 13. The observed maximum run-up height as a function of the averaged Froud number FRB. Solid line represents the linear long-wave theory for three types of wave generation.

This formula is similar that of the of a horizontal motion of a vertical wall (See A-7) in which $D^*=D$, and $\mathrm{FRB}=\mathrm{FR}=(L/\tau)/\sqrt{gD}$.

For $L^*>D/S$ (or $T<\tau$), the length scale relevant to the maximum run-up at the water's edge is D/S so that the average velocity of water waves is taken to be $\sqrt{gD}/2$. By putting $L^*=\tau\sqrt{gD}/2$, and $D^*=D$, the first relation of (7) is also written as (10) together with (9).

In the case of a vertical motion of a horizontal bottom of the scale b we may define the fictitious horizontal displacement L as $L=b\zeta_0/D$. The horizontal scale L^* can be expressed as $L^*=\tau\sqrt{gD}$ for $L^*<b$ and $L^*=b$ for $L^*>b$. Then the Froud number FRB is given by (9) and it follows that (10) is the formula for the maximum height H1 provided that D^* is replaced D (see A-3).

Thus, under the long wave approximation, three different types of wave generation can be formally expressed by the same relation (10), provided that D^* and FRB are suitably defined.

Experimental data is replotted in line with this relation in Fig. 13, and the coincidence of the data and the theory is good. But there exists a significant deviation from the theory for $S=1/10$, especially when $L=3$ cm or 6 cm. The major reason is believed to be a measuremental error of the instrument. As mentioned in the section 2, the maximum run-up is measured by thin stainless wires with a clearance of 5 mm from the sloping bottom, so that, if $S=1/10$, it measures the water level at the distance of 50 mm from the real water front, which is comparable to the horizontal displacements. Also the present theory does not take into account the effect of the bottom friction which is considered to be essential as the stroke and the slope become small.

6. Application to the estimation of tsunami run-up

The upper bound of the run-up of a tsunami due to the horizontal movement of the sloping bottom would be LS as shown in Fig. 12. However, to utilize a diagram like Fig. 12, it is necessary to estimate T, or, in other words, the horizontal scale of the displaced bottom, D/S, which, in practice, introduces some ambiguity. Therefore, it may be better to use Fig. 13 in which the maximum run-up height H1 can be estimated from the knowledge of the rise time τ and the horizontal displacement of the sloping bottom L, together with the bottom slope S.

Now, according to a simple fault model of earthquake (ABE, 1975) the approximate relation between a slip D_o(cm) on the fault and the earthquake moment M_0 (dyne-cm) is given by

$$D_o=10^{-7}\times M_0^{1/3}$$

The moment-magnitude M_w of the earthquake (KANAMORI, 1977) is defined by

$$M_w=(\log M_0-16.1)/1.5 \tag{11}$$

The relation between D_o and M_w becomes

$$\log D_0 = 0.5 M_w - 1.63. \tag{12}$$

Since the moment-magnitude M_w of the largest earthquake is supposed to be about 9.5, the maximum D_0 from (12) is about 15 m. The rise time of the earthquake faulting motion is believed to increase with the increase of the earthquake moment, and the mean speed of the crustal movement apart from the oscillating components seems to be in the range of a meter or so per second. Thus, we may put, $\tau = 15$ sec for $D_0 = 15$ m. If the horizontal displacement L is equated to D_0 and the slope S is 5×10^{-2}, the corresponding FRB is 0.54 and D^* is 1.38 m, so that, according to Fig. 13, H1 = 0.74 m ($LS = 0.75$ m). From this result, it is concluded that a purely horizontal displacement of a coastal bottom can generate only a small tsunami run-up even for great earthquakes as long as the bottom slope is small.

7. Concluding remarks

The major characteristic of the run-up at the water's edge is well described by a linear long-wave theory considering only the vertical component of the displacement. Since most of the bottom slope of the coastal sea region is less than 10^{-1}, purely horizontal displacement is found to be an inefficient mechanism to generate a tsunami.

In the numerical simulation of tsunamis based on the fault model of earthquake only the vertical component of the faulting motion is taken into account so far. But the vertical component of displacement due to horizontal bottom motion exists when the earthquake occurs in the region of the continental slope. It may be small, but it may modify the characteristics of the wave generated.

The maximum run-up for the three different types of wave generations can be expressed in one diagram as shown in Fig. 12 if the parameters of both axes are suitably defined. The ratio of the time T required for a disturbance to propagate the full range of the generating area to the rise time τ is essential. For a large $\tau (\tau \geq T)$, the ratio of the maximum run-up H1 to the vertical displacement ζ_0 increases with decreasing τ, but, there exists a lower bound of effective ζ_0 defined in connection with the size of the generating area and the speed of the wave generated. For $\tau \leq T$, $H1/\zeta_0$ remain constant except for the case of the horizontal motion of the vertical wall. Another expression equivalent to Fig. 12 is shown in Fig. 13 in which the relation of run-up height to other parameters is simpler than those of Fig. 12. Thus, for the estimation of the maximum run-up, this diagram is considered to be usuful.

A slight discrepancy is found between the theory and the experiment (see Fig. 10), but this discrepancy becomes smaller with decreasing slope of the moving bottom for $T/\tau > 1.0$. In view of the fact that waves generated in this experiment are beyond the range of linear shallow water wave, this discrepancy is thought to be originated in the assumption of linearity and hydrostatic state in theory. Thus, to lower the discrepancy, it seems necessary to calculate the wave form more rigorously either numerically or analytically.

8. Acknowledgement

The author wishes to express his hearty thanks to Prof. Kinjiro Kajiura for suggestions in various phases of this study. He also thanks Assoc. Prof. Isamu Aida and Dr. Tokutaro Hatori for useful comments and encouragement. Thanks are also given to Miss Ikuko Kato for typing the manuscript and Mr. Tokuji Nakano for making fantastic experimental equipments.

References

ABE, K., 1975, Reliable estimation on the seismic moment of large earthquakes, *J. Phycs. Earth*, **23**, 381-390.

DAS, M. M. and R. L. WIEGEL, 1972, Waves generated by horizontal motion of a wall, *J. Waterways, Harbors and Coastal Eng. Div.*, ASCE, **98** (WW1), 49-65.

GARCIA, W. J. J. JR., 1972, A study of water waves generated by tectonic displacement, *Univ. California Hydraulic Eng. Lab. Rep.*, HEL-16-9, 114 p.

HAMMACK, J. L., 1973, A note on tsunamis; their generation and propagation in an ocean of uniform depth, *J. Fluid Mech.*, **60**, 769-799.

KAJIURA, K., 1963, The leading wave of a tsunami, *Bull. Earthq. Res. Inst.*, **41**, 535-571.

KAJURA, K., 1970, Tsunami source, energy and directivity of wave radiation, *Bull. Earthq. Res. Inst.*, **48**, 835-869.

KANAMORI, H., 1977, The energy release in great earthquake, *J. Geophys. Res.*, **82**, 2981-2987.

LEE, Y. K. and LI-SAN HWANG, 1975, Waves generated by horizontal oscillations, *Tetra Tech Rep.*, Pasadena, Calif..

NODA, E., 1970, Water waves generated by landslides, *J. Waterways, Habors and Coastal Eng. Div.*, ASCE, **96** (WW4), 835-855.

TUCK, E. O. and LI-SAN HWANG, 1972, Long wave generation on a sloping beach, *J. Fluid Mech.*, **51**, 449-461.

URSELL, F., R. G. DEAN and Y. S. YU, 1959, Forced small-amplitude water waves: a comparison of the theory and experiment, *J. Fluid Mech.*, **7**, 33-52.

Appendix A

Tsunami Generation Models
—Vertical motion of a bottom in a channel of constant depth (type A)—

We take the origin of the Cartesian co-ordinate (x, y) at the still water level with the vertical axis y upwards. Consider a fluid domain bounded above by free surface, bounded below by a solid boundary and unbounded in the direction of wave propagation, i. e. $-\infty<x<\infty$, $-D<y<0$. Initially, the fluid is at rest with the free surface and the solid boundary. For $t>0$ the solid boundary is permitted to move.

The uniform movement of the horizontal bottom in the generating area delineated by $b>x>-b$ is given by

$$\zeta(x,t)=\begin{cases}\zeta_0(t/\tau), & \text{for } 0<t<\tau,\ |x|<b\\ \zeta_0 \quad , & \text{for } t>\tau,\ |x|<b\end{cases} \tag{A-1}$$

where τ denotes the rise time.

When, the horizontal bottom moves according to (A-1), the wave amplitude $\eta_l(x, t)$ from the still water level is given by

$$\eta_l(x,t)=(\zeta_0/\pi)(1/\tau)\int_{-\infty}^{\infty}\frac{\sin kb}{k}\frac{\cos(kx)}{\cosh(kD)}\times\left\{\frac{1}{\omega}\sin\omega t-H(t-\tau)\frac{1}{\omega}\sin\omega(t-\tau)\right\}dk \tag{A-2}$$

where $\omega^2=gk\tanh(kD)$, k denotes the wave number, H the Heaviside's step function.

We consider the maximum wave amplitude H at the center of the generating area, $x=0$. Assuming the long-wave approximation, (A-2) can be integrated straightforwardly as follows:

$$H/\zeta_0=\begin{cases}b/(\tau\sqrt{gD}), & \text{for } b<(\tau\sqrt{gD})\\ 1.0 \quad , & \text{for } b>(\tau\sqrt{gD})\end{cases} \tag{A-3}$$

(A-3) perfectly coincides with KAJIURA's solution (1970).

In the same fluid domain, HAMMACK (1973), not using the long-wave approximation, calculated the wave amplitude for two different types of bed motion, the exponential and half-sine types. For example, the half-sine type of bed motion $\zeta_s(x, t)$ is given by

$$\zeta_s(x,t)=\begin{cases}\frac{\zeta_0}{2}\left\{1-\cos\frac{\pi t}{\tau}\right\}, & \text{for } 0<t<\tau,\ |x|<b\\ \zeta_0 \quad , & \text{for } \tau<t \ ,\ |x|<b.\end{cases} \tag{A-4}$$

For the case of $b/\zeta_0\gg1.0$, the maximum wave armplitude at $x=0$ for the case of the half-sine bed motion is shown in Fig. A-1, in which the solution (A-3) is also included. For $b>(\tau\sqrt{gD})$, both solutions perfectly coincide. Therefore the long-wave approximation is valid and the time dependence of the bottom motion is irrelevant for the maximum run-up

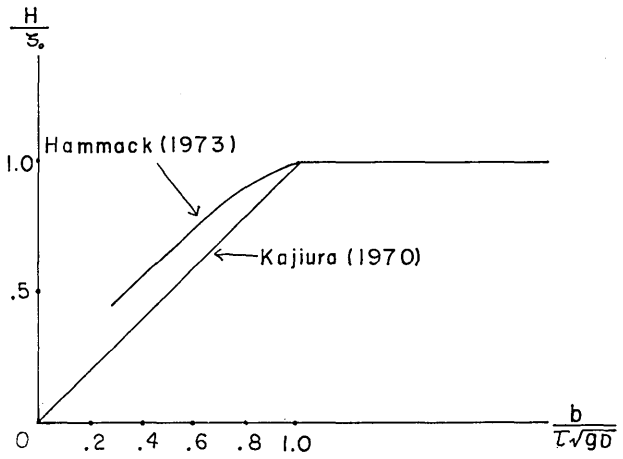

Fig. A-1. Solutions of KAJIURA (1970) and HAMMACK (1973) for the vertical motion of a bottom in an ocean of constant depth (type A). KAJIURA assumed the long-wave approximation and the time dependence of the bed motion is linear. Hammack did not assume the long-wave approximation and the bed motion is half-sine type (for $b/\zeta_0 \gg 1.0$).

at $x=0$, provided the size of the generating area is much greater than the water depth.

—Horizontal motion of a vertical wall (type B)—

Consider a similar fluid domain mentioned above, but a vertical wall is situated at $x=0$, i. e.. we consider only $0<x<\infty$. When the vertical wall moves horizontally, the wave amplitude $\eta(x, t)$ from the still water level is given by (NODA, 1970)

$$\eta(x,t) = -\left(\frac{2}{\pi}\right)\cdot\int_0^\infty dk\int_0^t d\tau_1 \times\int_0^{-D}\frac{\cos\omega(t-\tau_1)\cdot\cosh k(y+D)\cdot\cos kx}{\cos(kD)}F(y,\tau_1)dy \qquad \text{(A-5)}$$

where $F(y, \tau_1)$ represents the time and y dependence of horizontal velocity of the wall.

We assume $F(y, \tau_1)$ as

$$F(y,\tau_1)=\begin{cases}(L/\tau) & \text{for } 0<\tau_1<\tau\\ 0 & \text{for } \tau<\tau_1\end{cases} \qquad \text{(A-6)}$$

Substituting (A-6) for (A-5) and using the long-wave approximation, the maximum wave amplitude H from the still water level at $x=0$ is given by

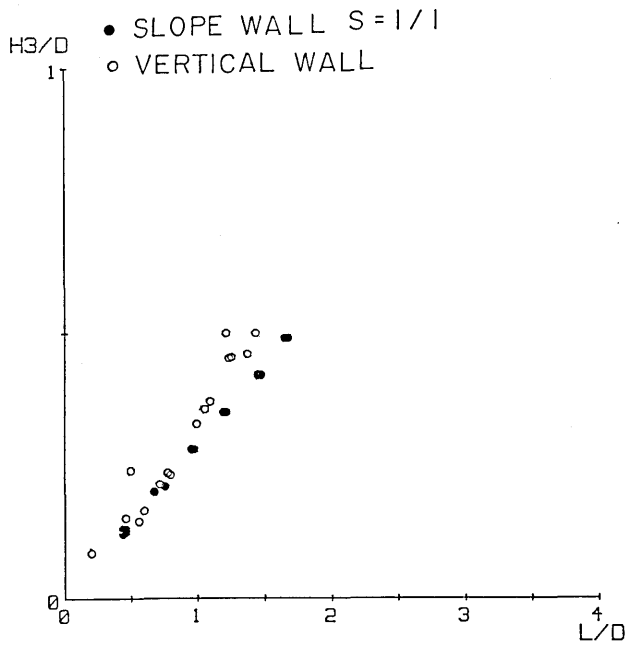

Fig. B-1. Nondimensional plots of the maximum wave amplitude at a location downstream 15D from the wall for S=1/1 and for a vertical wall as a function of the stroke (both are normalized by water depth D). The data is taken from GARCIA (1972).

$$H/D=L/(\tau\sqrt{gD})=FR \tag{A-7}$$

Without the long-wave approximation, the equation (A-5) is integrated numerically and shown in Fig. 12.

Appendix B

As shown in Fig. 5, the wave for the case of $S=1/1$ exhibits analogous characteristics to the wave generated by the horizontal motion of a vertical wall.

Fig. B-1 is a non-dimensional plot of the maximum wave amplitude at a location downstream from the wall for $S=1/1$ and for a vertical wall as a function of the horizontal displacement L after GARCIA (1972) (both are normarized by the water depth D). This data shows an analogous tendency with respect to L/D. Since wave characteristics are found analogous in both near and far fields, we may infer the wave characteristics for a vertical wall motion from those of the $S=1/1$ case as least to the order of accuracy found in the figure.

12. 海底斜面の水平な動きにより発生する津波の実験的研究

地震研究所 岩 崎 伸 一

海底斜面の水平な動きによる津波を実験的に議論した．実験は，地震研究所地下実験水槽を用い，3つの独立なパラメーター，S, L, τ を変化させて行なった．S は傾斜壁の傾きであり，L は水平変位，τ は立ち上がり時間である．最大はい上り高に関して，以下の事実が明らかになった．

1) $S=1/1$ の場合，最大はい上がり高は，鉛直壁の水平な動きによるものと，同様の傾向を示す．
2) $S\leq 1/3$ では，最大はい上がり高は，変位の鉛直成分 LS に支配される．
3) 発生した波の性質は，線型長波理論でよく記述される．
4) 3つの異なる波の発生機構，一様水深海底の鉛直変位モデル，鉛直壁の水平変位モデル，傾斜壁の水平変位モデルに関して，統一的な解釈が可能である．